Computing Different Modes on Cathodes of DC Glow and High-Pressure Arc Discharges: Time-Dependent Versus Stationary Solvers

Pedro G. C. Almeida, Mikhail S. Benilov,* Mário D. Cunha, José G. L. Gomes

Complex behavior can appear in the modeling of gas discharges even in apparently simple steady-state situations. Time-dependent solvers may fail to deliver essential information in such cases. One of such cases considered in this work is the 1D DC discharge. The other case is represented by multiple multidimensional solutions existing in the theory of DC discharges and describing modes of current transfer with different patterns of spots on the cathodes. It is shown that, although some of the solutions, including those describing beautiful self-organized patterns, can be computed by means of a time-dependent solver, in most examples results of time-dependent modeling are at best incomplete. In most examples, numerical stability of the time-dependent solver was not equivalent to physical stability.

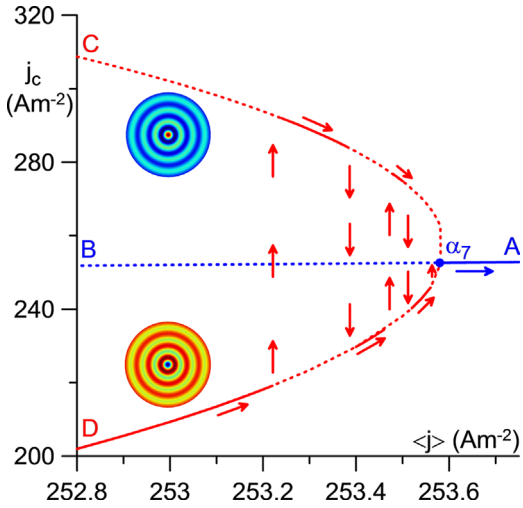

1. Introduction

DC gas discharges are usually computed by means of time-dependent solvers: an initial state of a discharge is specified and its evolution over time is followed until a steady state has been attained. This is the approach used by virtually all popular toolkits for computer modeling of gas discharges, although exceptions exist: e.g., toolkit Plasimo[1] supports both transient and steady-state simulations.

M. S. Benilov, P. G. C. Almeida, M. D. Cunha, J. G. L. Gomes
Departamento de Física, FCEE, Universidade da Madeira, Largo do Municipio, 9000 Funchal, Portugal
E-mail: benilov@uma.pt
P. G. C. Almeida, M. S. Benilov, M. D. Cunha, J. G. L. Gomes
Instituto de Plasmas e Fusão Nuclear, IST, Universidade de Lisboa, Lisbon, Portugal

One of the limitations of such approach is illustrated by Figure 1, where results are shown of numerical solution of one of the simplest problems of gas discharge theory, namely, of the problem of one-dimensional (1D) DC glow discharge. The plasma-producing gas is argon at the pressure of 120 Torr, the interelectrode gap is 0.5 mm, the kinetic and transport coefficients used in the simulations are specified in Appendix A (note that this work is concerned with the methodology of computing solutions; questions related to the experimental realization, such as the possibility of glow to arc transition at high current densities shown in Figure 1, are not considered). The points in Figure 1 represent the current-voltage characteristic (CVC). These data have been computed with the use of the Plasma module of COMSOL Multiphysics employed as illustrated by the DC glow discharge model from its model library. The simulations in Figure 1 started from a high value of discharge voltage U and then U was gradually reduced; each computed steady state served as an initial

© 2016 WILEY-VCH Verlag GmbH & Co. KGaA, Weinheim

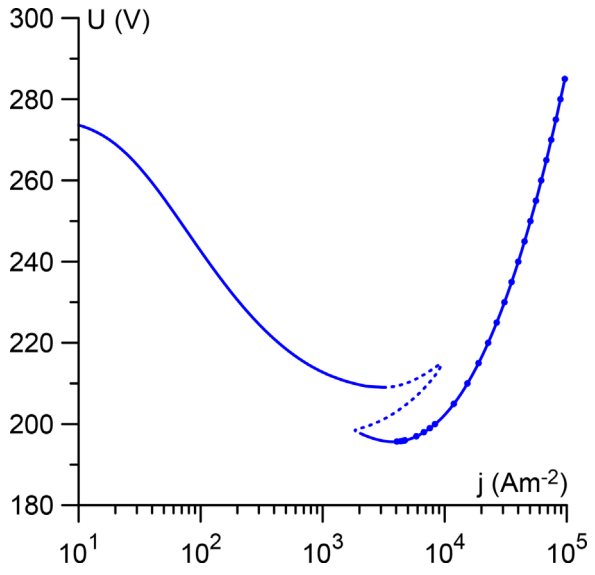

Figure 1. CVC of the 1D DC glow discharge in Ar. Points: plasma module of COMSOL Multiphysics. Solid: plasma module with control of current. Dotted: stationary solver.

condition for the computation of the next state. The convergence was lost shortly before the minimum of the CVC.

Thus, the straightforward application of the Plasma module of COMSOL Multiphysics allows one to readily compute only the abnormal discharge. A more robust code can be built by adding the possibility of using the discharge current density j as a control parameter (instead of the discharge voltage U). This may be achieved by supplementing the Plasma module by a boundary condition written with the use of the "weak form" formulation available in COMSOL, without expressly introducing a ballast resistance. The solid lines in Figure 1 depict results obtained in this way by starting from high and low values of the current density. The results are discontinuous, which is why the lines are disconnected; as the code has reached the end of one of the lines, it jumped to the other line.

Presumably, the two solid lines in Figure 1 represent branches of the same discharge mode which manifests hysteresis. Such hysteresis is unusual in a 1D DC discharge, but the alternative – which is the existence of two disconnected modes – would be unusual as well. It is desirable to clarify this point.

To this end, a replica of the Plasma module was built with the use of the weak form formulation. This formulation allows one to employ a stationary solver (and also to introduce some other relevant modifications, in particular, to more accurately evaluate boundary conditions and the current density in the calculation domain and at the boundaries and to remove the restriction that does not allow the user to set diffusion coefficients of heavy particles).

The code built in this way works well for all the conditions of Figure 1 and the results are depicted by the dotted line (most of the line coincides with the solid lines and only a part is visible). One can see that the transition between low and high currents or, in other words, between subnormal and abnormal discharge is accompanied by hysteresis occurring in a rather wide current range, $3\,\mathrm{kAm^{-2}} \lesssim j \lesssim 9\,\mathrm{kAm^{-2}}$. We do not discuss here the underlying physics because of lack of space and only mention that a similar hysteresis has been found by means of the stationary solver in the xenon plasma[2]; however, modeling results not shown here reveal that the disregard of stepwise ionization does not result in the disappearance of the hysteresis in Ar, in contrast to what happens for Xe.

This example shows that complex behavior can appear in the modeling of gas discharges even in apparently simple steady-state situations and time-dependent solvers may fail to deliver essential information in such cases.

Another example of complex behavior is represented by modes with different patterns of spots on cathodes of DC discharges. Such modes do not necessarily result from different physical mechanisms: if a spot or pattern is unrelated to non-uniformities of the electrode surface, then it is a manifestation of self-organization. Hence, self-consistent theoretical models of current transfer to cathodes of DC discharges, even the most basic ones, should admit multiple multidimensional solutions, which exist at the same discharge current and describe a spotless mode and modes with spots or spot patterns; see review.[3]

In the theory of high-pressure DC arc discharges, such solutions have been computed with the use of stationary solvers of ANSYS and COMSOL software (e.g., refs.,[4,5–8] respectively) and a home-made stationary solver.[9] Stationary solvers of COMSOL Multiphysics have been employed for computing solutions describing different modes of current transfer in the theory of DC glow discharges.[3] On the other hand, some multiple steady-state solutions describing different modes of current transfer to electrodes of DC discharges have been computed in the course of time-dependent modeling,[10–14] although the reported solutions refer to just one current value or a narrow current range. Note that solutions periodic in time describing self-organized patterns in DBDs have been successfully computed by time-dependent solvers; e.g., ref.[15]

In this situation, the question if time-dependent solvers are suitable for investigation of complex behavior of DC gas discharges, illustrated by Figure 1, arises again. In other words, can solutions describing different modes of current transfer to cathodes of DC discharges be systematically computed in a wide current range by means of time-dependent solvers? In addition to being of methodological interest, this question is relevant for applications, e.g., for modeling of cathode arc spots. One of the objectives of this

© 2016 WILEY-VCH Verlag GmbH & Co. KGaA, Weinheim

work is to try to answer this question, considering as an example time-dependent solvers of COMSOL Multiphysics. The other question to be dealt with concerns stability is the (im)possibility of computing a steady state of a gas discharge by means of a time-dependent solver a proof of (in)stability of this state, as is frequently assumed?

In this work, both low-current, cold-cathode DC (glow) discharges, and high-current, hot-cathode DC (arc) discharges are considered. Note that despite the different physical mechanisms of electron emission in the two discharges, the pattern of self-organization is the same; *cf.*[3]

The outline of the paper is as follows. The models used in this work and relevant aspects of numerical realization on the COMSOL Multiphysics platform are briefly described in Section 2. In Sections 3.1 and 3.2, examples of simulation results are given for, respectively, high-pressure arc discharge and glow discharge. A summary and conclusions are given in Section 4.

2. Models and Numerics

2.1. High-Pressure Arc Discharge

Plasma-cathode interaction in high-pressure DC arc discharges is simulated in this work by means of the so-called model of nonlinear surface heating, which was proposed for the first time apparently in ref.[16] and has become a standard simulation tool by now; e.g., refs.[17,18] The model is based on the fact that a very substantial electric power is deposited by the arc power supply into the near-cathode space-charge sheath, so the energy flux to the cathode surface is generated in a very thin near-cathode plasma layer comprising the space-charge sheath and the adjacent ionization layer. As a consequence, the plasma-cathode interaction is to the first approximation unaffected by the arc column and may be simulated independently.

The procedure may be briefly described as follows. First, one solves 1D equations describing current transfer through the near-cathode plasma layer, thus calculating all parameters of the near-cathode layer as functions of the local temperature T_w of the cathode surface and of the near-cathode voltage drop U. In particular, densities of the energy flux and the electric current from the plasma to the cathode surface are determined: $q = q\,(T_w, U)$ and $j = j\,(T_w, U)$.

At the second step, distribution of temperature and potential inside the cathode body and at the surface are calculated by means of solving the thermal-conduction and current-continuity equations in the cathode. The boundary conditions at the current-collecting part of the cathode surface are $\kappa\partial T/\partial n = q\,(T_w, U)$ and $\sigma\partial\varphi/\partial n = j\,(T_w, U)$, where κ and σ are thermal and electrical conductivities of the cathode material, n is a direction locally orthogonal to the cathode surface and directed outside the cathode, and $q\,(T_w, U)$ and $j\,(T_w, U)$ are the dependences found at the first step. After the solution has been found, one will know distributions of the temperature T_w and, consequently, of all parameters of the near-cathode layer along the cathode surface. Integrating the distribution of the current density found in this way, one will find the value of the arc current I corresponding to the specified near-cathode voltage U.

In order to best illustrate the comparison of different solvers, it is desirable to consider a simple geometry which admits temperature distributions of different symmetries: a cathode in the form of a upright cylinder with the top in contact with the plasma, the bottom being externally cooled, and the lateral surface being electrically and thermally insulated.

Numerical results reported in this work refer to arcs burning in argon and cathodes made of tungsten. The near-cathode plasma layer was calculated by means of the formulas summarized in ref.[19] Data on thermal conductivity and emissivity of tungsten have been taken from refs.,[20,21] respectively.

2.2. Glow Discharge

We consider the conventional model of glow discharges, which comprises equations of conservation of the ions and the electrons, transport equations for the ions and the electrons written in the drift-diffusion approximation, and the Poisson equation. Boundary conditions at the electrodes are written in the conventional form as well: diffusion fluxes of the attracted particles are neglected compared to drift; the normal flux of the electrons emitted by the cathode is related to the flux of incident ions in terms of the effective secondary emission coefficient, which is assumed to characterize all mechanisms of electron emission (due to ion, photon, and excited atom bombardment)[22]; density of the ions vanishes at the anode; the normal component of the electric current density vanishes at the insulating walls of the discharge vessel.

Once again, in order to best illustrate the comparison of different solvers we consider a simple geometry which admits solutions of different symmetries: the discharge tube in the form of a upright cylinder with parallel-plane electrodes and lateral (insulating) wall reflecting impinging charged particles back to the discharge. The latter amounts to the boundary conditions for the charged particle densities at dielectric surface being zero normal derivatives.

Results reported in this work refer to plasmas of xenon and argon. The kinetic and transport coefficients used in the modeling are specified in the beginning of Section 3.2 and in Appendix A, respectively.

© 2016 WILEY-VCH Verlag GmbH & Co. KGaA, Weinheim

2.3. Numerical Realization

Let us introduce cylindrical coordinates (r, ϕ, z) with the z-axis coinciding with the axis of the cathode or the discharge tube (in the cases of arc cathodes or DC glows, respectively). The boundary-value problems discussed in the preceding sections admit solutions of different symmetries: a 1D solution $f = f(z)$, describing the spotless (diffuse) mode of current transfer to the cathode; axially symmetric, or 2D, solutions $f = f(r, z)$, describing modes with a spot at the center of the cathode and/or one or more ring spots; and three-dimensional (3D) solutions $f = f(r, \phi, z)$, describing modes with one or more off-center spots.

The 3D solutions are periodic with respect to the azimuthal angle. For example, a solution with two spots at the edge of the cathode has a period of π and can be computed on the computation domain $0 \leq \phi \leq \pi/2$ with the boundary conditions of zero derivatives $\partial f/\partial \phi$ at $\phi = 0$ and $\phi = \pi/2$. Such reduction of the computation domain, in addition to loosening the requirements for RAM and CPU time, also reduces the number of multiple solutions to which the code can converge: in this example, solutions with, e.g., one or three spots at the edge of the cathode are eliminated. Note, however, that the outcome of calculations is still not unique: sometimes the code converges not to the desired solution with two spots, but to a solution with, e.g., four, or six, or eight spots, if such solutions exist under conditions specified.

One of the objectives of this work is to compare capabilities of time-dependent and stationary solvers of COMSOL Multiphysics to systematically compute different modes of current transfer to cathodes of DC discharges in a wide current range. To this end, we attempt to recompute by means of a time-dependent solver some of solutions which describe different modes and have been computed in preceding works by means of the stationary solver.

The boundary condition mentioned in the Introduction was used, which adds the possibility of running the code for specified values of the discharge current I, with the corresponding values of U being found as a part of the solution jointly with distributions of all parameters $f(r, \phi, z)$ (we remind that U is the near-cathode voltage drop in the case of high-pressure arcs and the discharge voltage in the case of DC glows).

The equations in the cathode in the modeling of plasma-cathode interaction in high-pressure arc discharges were solved by means of Heat Transfer in Solids module of COMSOL Multiphysics. A module for computation of current transfer through the near-cathode plasma layer was written in Fortran. Numerical data on the functions $q(T_w, U)$ and $j(T_w, U)$, produced by the latter module, were interpolated by means of two-dimensional (2D) bi-cubic spline in MATLAB, which interacted with COMSOL via Livelink.

Simulations of glow discharge reported in Section 3.2 have been performed with the use of the modules Transport of Diluted Species and Electrostatics of COMSOL Multiphysics.

2.4. Stability of Steady States

It is frequently implied that time-dependent solvers compute states of DC discharges which are stable, so no special investigation of stability of these states is needed, in contrast to what happens if a stationary solver has been employed. However, in reality, the situation is more complex. First, one could hope (at best) for the computed solutions to be stable only against perturbations having the same symmetry to which the code is adjusted. For example, states computed by means of an axially symmetric time-dependent solver may be unstable against 3D perturbations, which are usually just the most dangerous ones.

Second, even if consideration is limited to perturbations having the symmetry to which the code is adjusted, the question arises if numerical stability of time-dependent solvers commonly used in the modeling of gas discharges is equivalent to physical stability or, in other words, if time-dependent solvers can compute all stable states and will not compute any unstable state.

An objective of this work is to try to answer this question. To this end, results given by time-dependent solvers of COMSOL Multiphysics will be analyzed in light of information on stability of different steady states, which has been obtained in previous works in the framework of the linear stability theory, analytically and by means of the eigenvalue solver of COMSOL for arc cathodes[23,24] and by means of the COMSOL eigenvalue solver for axially symmetric states of DC glows.[25]

3. Results

Multiple steady-state solutions existing in the considered problems for the same values of the discharge current have been computed in preceding works by means of stationary solvers. The pattern of these solutions and physics behind them have been relatively well understood by now and are discussed in detail elsewhere; see ref.,[3] where also a discussion of experimental verification of these solutions can be found. In this work, the treatment is focused on which of these solutions can be computed by means of time-dependent solvers and how the results of these calculations relate to the known stability properties of the solutions.

Solid and dotted lines in the figures of this section represent results obtained by means of time-dependent and stationary solvers, respectively. Simulations by means

© 2016 WILEY-VCH Verlag GmbH & Co. KGaA, Weinheim

of time-dependent solvers, if successful, give results coinciding with those given by the stationary solver; therefore, there is a dotted line present beneath each solid line. For example, solid lines a_1A and CD in Figure 2 are superimposed over parts of the dotted lines Ba_1A and CDa_1.

Each one of the multiple steady-state solutions is a continuous function of current, although not necessarily single-valued; a solution may join another solution (a bifurcation) or turn back but cannot just disappear. For example, in Figure 2 the solution CDa_1 turns back at the turning point D and joins the solution Ba_1A at the bifurcation point a_1 (both points are marked by circles). Therefore, each dotted line in each figure is continuous and either represents a loop or is limited by the boundaries of the figure or by bifurcation points, although some sections of dotted lines may be invisible because of being superimposed by solid lines as mentioned above.

3.1. High-Pressure Arc Discharge

Examples of calculations of different modes of current transfer to cathodes of high-pressure arc discharge are shown in Figures 2–4. The pressure of plasma-producing gas (argon) here is set equal to 1 bar, the cathode radius is 2 mm and height 10 mm, and the temperature at the bottom of the cathode is 293 K.

The CVC of the diffuse mode and the first 3D mode are shown in Figure 2. Note that both modes were computed by the same code, which means that the diffuse mode, which is 1D, was computed in the 3D domain. The 3D mode is

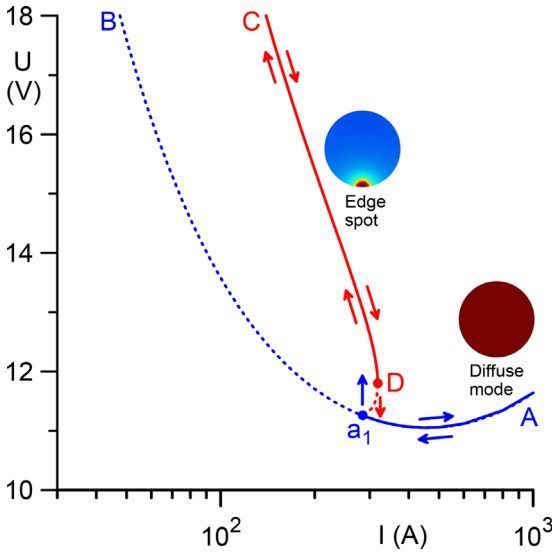

Figure 2. CVC of the diffuse mode ($B\alpha_1A$) and the first three-dimensional mode (CDa_1) of current transfer to the cathode of a high-pressure arc discharge. Conditions listed in the beginning of Section 3.1.

associated with a spot at the edge of the cathode. The 3D mode branches off from the diffuse mode at the bifurcation point a_1 in the direction of higher currents, then it turns backward at the turning point D and continues in the direction of lower currents; see ref.[3] for discussion.

Two series of simulations by means of the time-dependent solver have been performed as is schematically indicated by arrows in Figure 1. In the first series, simulations started from high currents, namely, from state A belonging to the diffuse mode. As the current was successively decreased, the time-dependent solver first continued along the diffuse mode. When the current has been reduced down to the value corresponding to the bifurcation point a_1, the solver jumped to the 3D mode and then continued along it.

The second series of simulations started from state C on the 3D mode. As the current was successively increased, the time-dependent solver continued along the 3D mode until the turning point D has been reached. At the turning point, the solver jumped to the diffuse mode and then continued along it.

Thus, the time-dependent solver is capable of computing steady states belonging to the section a_1A of the diffuse mode and to the section CD of the 3D mode with the spot at the edge. This behavior conforms to results of stability analysis: these are the only stable states, as shown analytically[23] and numerically[24] in the framework of the linear stability theory. The existence of hysteresis, suggested by the time-dependent modeling and seen in Figure 2, agrees with the linear stability theory [23,24] and the experiment (e.g., ref.[26]).

The lines $B\alpha_1A$ and $E\alpha_1GF$ in Figure 3 depict CVCs of the diffuse mode and the first 2D mode, respectively. Here, the diffuse mode was computed in the 2D domain. The state α_1 represents the bifurcation point at which the 2D mode branches off from the diffuse mode. The 2D mode comprises two branches separated by the bifurcation point: the branch $E\alpha_1$, associated with a ring spot at the edge of the cathode, and the branch α_1GF, which is associated with a spot at the center of the cathode and possesses a turning point (G). Note that the CVC of the branch $E\alpha_1$ coincides to the graphic accuracy with the section $B\alpha_1$ of the CVC of the diffuse mode.

Because of the latter, the graphic representation of different modes seen in Figure 3 is not very clear. A more illustrative representation is shown in Figure 4, where j_e is the current density at the edge of the cathode.

When the simulations started from high currents, namely, from state A on the diffuse mode (Figures 3a and 4a), the time-dependent solver followed the diffuse mode till approximately the bifurcation point α_1, then jumped to the branch with a spot on the center and continued along this branch. When the simulations started from low currents on the branch with a spot on the center

© 2016 WILEY-VCH Verlag GmbH & Co. KGaA, Weinheim

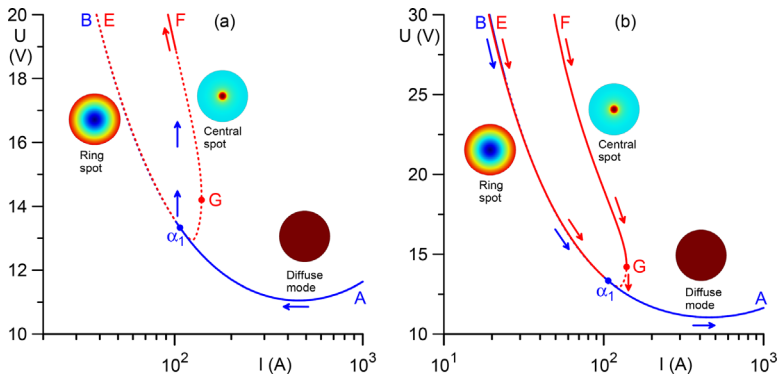

Figure 3. CVC of the diffuse mode ($B\alpha_1A$) and the first 2D mode ($E\alpha_1GF$) of current transfer to the cathode of a high-pressure arc discharge. Time-dependent simulations (solid) started from high (a) and low (b) currents.

(state F; Figures 3b and 4b), the time-dependent solver followed this branch till the turning point G, then jumped to the diffuse mode and followed it. This behavior conforms to results on stability of different modes against 2D perturbations[23,24]: the only 2D steady states stable against 2D perturbations are those belonging to the section α_1A of the diffuse mode and section FG on the central-spot branch of the first 2D mode.

On the other hand, the time-dependent solver produced converged solutions in simulations that started from low currents on the branch with a ring spot (state E; Figures 3b and 4b): the solver followed this branch till the end (state α_1) and then continuously switched to the diffuse mode and followed the latter. Furthermore, the time-dependent solver produced converged solutions also in simulations that started from low currents on the diffuse mode (state B; Figures 3b and 4b): the solver followed this branch till the state $I = 24$ A, then jumped to the ring-spot branch and followed it till the bifurcation point α_1, and then continuously returned to the diffuse mode and followed the latter.

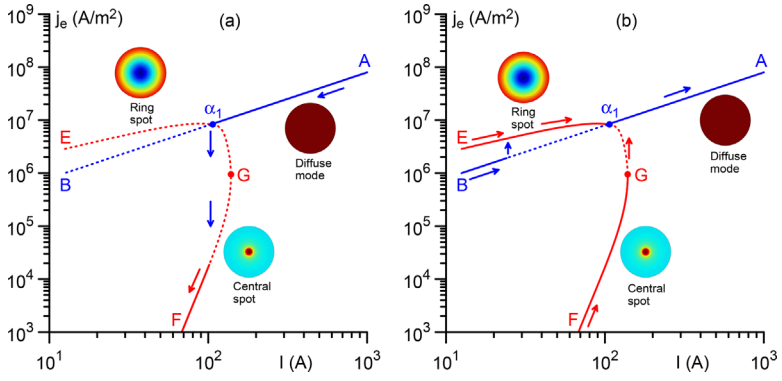

Figure 4. Graphic representation of the diffuse mode ($B\alpha_1A$) and the first 2D mode ($E\alpha_1GF$) of current transfer to the cathode of a high-pressure arc discharge. j_e: current density at the edge of the cathode. Time-dependent simulations (solid) started from high (a) and low (b) currents.

This behavior is in clear contradiction with the linear stability theory: all steady states on the ring-spot branch $E\alpha_1$ and the section $B\alpha_1$ of the diffuse mode are unstable against 2D perturbations.

3.2. Glow Discharge

Once again, in order to best illustrate the comparison of different solvers, we consider in this section a simple example: the most basic self-consistent model of glow discharge, which comprises a single ion species (molecular ions) and a single ionization channel (direct ionization), with electron kinetic and transport coefficients depending only on the local electric field (the so-called local-field approximation). While being relatively simple, this model nevertheless provides a representative example: an account of detailed plasma chemistry and non-locality of electron kinetics results in an increase in the number of multiple solutions but does not change their pattern.[2]

Results shown in Figures 5 and 6 refer to the plasma-producing gas being xenon at the pressure of 30 Torr (here $\langle j \rangle$ designates the average current density at the cathode surface). The transport and kinetic coefficients are the same as in ref.,[27] the effective secondary emission coefficient is 0.33, the interelectrode gap is 0.5 mm, the discharge tube radius is 1.5 mm in 2D simulations and 0.5 mm in 3D simulations. The lines $B\beta_1b_8a_8\alpha_1A$ and $\beta_1C\alpha_1D\beta_1$ in Figure 5 represent CVCs of the 1D mode and the first 2D mode, respectively. In the case of glow discharge, each 2D mode joins the 1D mode at two bifurcation points; for the first 2D mode, the bifurcation points are designated α_1 and β_1. As in the case of high-pressure arc, the 2D mode comprises two branches separated by the bifurcation points: the branch $\beta_1D\alpha_1$, associated with a ring spot at the edge of the cathode, and the branch $\beta_1C\alpha_1$, associated with a spot at the center.

In contrast to what happens in the more detailed model to which Figure 1 refers, in this case, the 1D mode reveals no retrograde behavior (hysteresis) and there is no problem in computing it in the 1D domain by means of the time-dependent solver in the whole range of its existence, from A to B (high to low currents) and B to A (low to high currents). The same is true also for computation performed in the 2D domain, in spite of this mode being unstable against 2D perturbations between the bifurcation

© 2016 WILEY-VCH Verlag GmbH & Co. KGaA, Weinheim

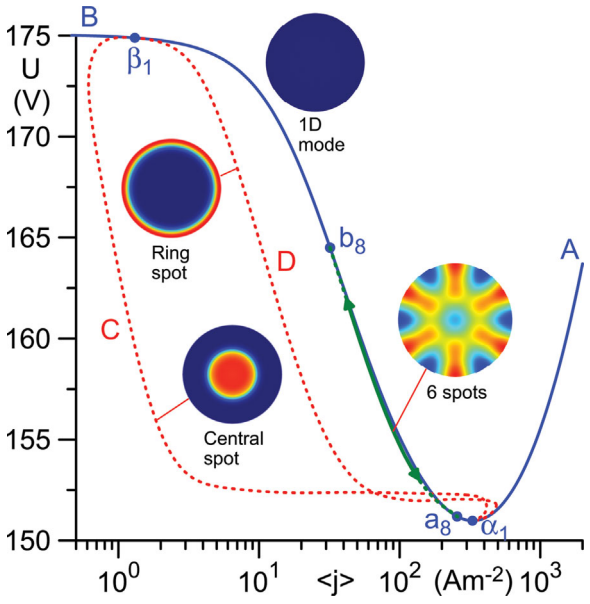

Figure 5. CVCs of different modes of DC glow discharge in Xe. $B\beta_1 b_8 a_8 \alpha_1 A$: the 1D mode. $\beta_1 C \alpha_1 D \beta_1$: the first 2D mode. $a_8 b_8$: the eighth three-dimensional mode.

points α_1 and β_1.[25] On the other hand, the time-dependent solver does not allow computation of any state belonging to the 2D mode.

Line $b_8 a_8$ in Figure 5 depicts the eighth 3D mode, which is associated with a pattern of six spots forming a ring, and is barely distinguishable from the line $B\beta_1 b_8 a_8 \alpha_1 A$ representing the 1D mode. The time-dependent solver allows one to compute a section of this mode (this section is shown by the solid line ending with arrows) but not the mode in the entire range of its existence.

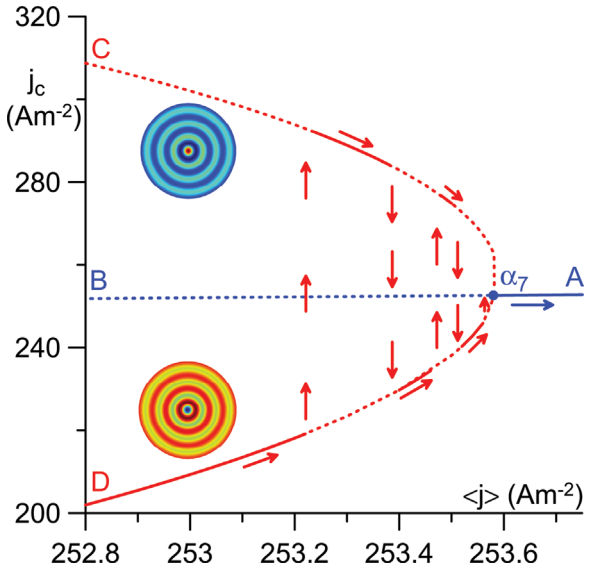

Figure 6. Graphic representation of the 1D ($B\alpha_7 A$) and seventh 2D ($C\alpha_7 D$) modes of DC glow discharge in Xe. j_c: current density at the center of the cathode. Time-dependent simulations started from state *D*.

As an example of a higher order 2D mode, the 7th 2D mode of DC glow discharge is depicted in Figure 6 by the line $C\alpha_7 D$. Since the CVC of this mode is indistinguishable from that of the 1D mode, the coordinates $(\langle j \rangle, j_c)$ are chosen, where j_c is the current density at the center of the cathode. This mode comprises branches with a central spot and three ring spots inside the cathode (line $C\alpha_7$) and three ring spots inside the cathode and a ring spot at the periphery ($D\alpha_7$). The time-dependent simulations started from the state D on the branch associated with a pattern without a central spot and then $\langle j \rangle$ was increased with a step of 0.02 Am^{-2}. As seen in Figure 6, the time-dependent solver jumped erratically between the two branches of the seventh 2D mode until it finally jumped to the 1D mode $B\alpha_7 A$ and stayed on it. Thus, the time-dependent solver produces a fragmentary picture: a patch of solution here and another there, and one would have difficulties even in realizing that the patches belong to the same mode. Note that results not shown here reveal that, depending on the step in the average current density, the time-dependent solver may also jump to other modes or stop converging.

If the lateral wall of the discharge tube absorbs (rather than reflects) the ions and the electrons, the boundary conditions of zero normal derivatives of the densities of the charged particle at the wall are replaced with the zero density conditions. As a consequence, the problem does not admit a 1D solution. Skipping detailed results for lack of space, we only note the following. The simplest discharge mode in this case is the 2D mode comprising the (2D) Townsend discharge at low currents, the subnormal discharge and discharge with the normal spot at intermediate currents, and the abnormal discharge at high currents. The CVC of this mode is shown in Figure 2 of ref.[25] and is similar to those computed in previous works by means of time-dependent solvers (e.g., Figure 1[28] and Figure 2[29]), except for the small retrograde section connecting the Townsend and subnormal discharges and denoted $a^{(2)}a^{(3)}$ in above-mentioned figure. The time-dependent solver cannot compute the retrograde section. However, it is able to compute all the rest of the mode, and this is again in contradiction with the linear stability theory: there is a wide current range ($a^{(1)}a^{(4)}$ in the above-mentioned figure) where all steady states are unstable against 2D perturbations.[25]

4. Concluding Remarks

Complex behavior can appear in the modeling of gas discharges even in apparently simple steady-state

© 2016 WILEY-VCH Verlag GmbH & Co. KGaA, Weinheim

Table 1. Kinetic scheme for argon and data used to describe each process.

$Ar + e^- \rightarrow Ar^+ + e^- + e^-$	BOLSIG+[30,31]
$Ar^* + e^- \rightarrow Ar^+ + e^- + e^-$	Equation (8)[32]
$Ar_2^* + e^- \rightarrow Ar_2^+ + e^- + e^-$	$9 \times 10^{-8} T_e^{0.7} e^{-3.66/T_e} cm^3 s^{-1}$[33]
$Ar + e^- \leftrightarrows Ar^* + e^-$	BOLSIG+[30,31]
$Ar^+ + Ar + Ar \rightarrow Ar_2^+ + Ar$	$2.5 \times 10^{-31} cm^6 s^{-1}$[33]
$Ar^* + Ar^* \rightarrow Ar^+ + Ar + e^-$	$10^{-9} cm^3 s^{-1}$[33]
$Ar_2^+ + e^- \rightarrow Ar^* + Ar$	$5.38 \times 10^{-8} T_e^{-0.66} cm^3 s^{-1}$[33]
$Ar^* \rightarrow Ar + \phi$	$7.00 \times 10^8 s^{-1}$[34]
$Ar_2^* \rightarrow 2Ar + \phi$	$3.5 \times 10^5 s^{-1}$[34]
$Ar^* + Ar + Ar \rightarrow Ar_2^* + Ar$	$1.0 \times 10^{-32} cm^6 s^{-1}$[34]

T_e in eV.

situations and time-dependent solvers may fail to deliver essential information in such cases. One of such cases considered in this work is the 1D DC discharge in argon; Figure 1.

The other case is represented by multiple multidimensional solutions existing in the theory of DC discharges and describing modes of current transfer with different patterns of spots on the cathodes. We attempted to recompute by means of time-dependent solvers of COMSOL Multiphysics some of such solutions computed in preceding works by means of the stationary solver for both glow and high-pressure arc discharges. Of all the modes considered, only one could be computed in the whole region of its existence without gaps by means of the time-dependent solver: the 1D mode of DC glow discharge in xenon in the framework of the local-field approximation; line $B\beta_1 b_8 a_8 \alpha_1 A$ in Figure 5. No states belonging to some modes could be computed by means of time-dependent solvers; e.g., the first 2D mode in glow discharge in xenon, line $\beta_1 C \alpha_1 D \beta_1$ in Figure 5. In all the other cases, the modeling results are incomplete. An extreme example of the latter situation is seen in Figure 6: the time-dependent solver has produced a patchy picture, and one would have difficulties even in understanding which patch belongs to which mode.

On the contrary, the stationary solver is capable of computing all modes in the whole range of their existence and is, therefore, a tool of choice for investigation of the whole pattern of solutions in a wide current range. Of course, there are also numerical aspects not discussed here: the use of stationary solvers is generally simpler than the use of time-dependent solvers, since there is more freedom in the choice of spatial mesh and no necessity to resolve different time scales.

It is frequently understood that no special investigation of stability of steady states computed by means of time-dependent solvers is needed, since time-dependent solvers compute states which are stable and only such states (Table 1). The latter proved true in only one of the examples considered; Figure 2. In all the other cases where linear stability results are known, time-dependent solvers have computed some states that are unstable and/or were unable to compute some stable states. In other words, numerical stability of time-dependent solvers of COMSOL is not necessarily equivalent to physical stability. Furthermore, time-dependent solvers cannot give any information concerning stability against perturbations of symmetries different from the one to which the solver is adjusted. For example, 2D states with the spot at the center of the cathode computed by the time-dependent solver in 2D under conditions of Figure 3a are unstable against 3D perturbations.[23,24] Consequently, conclusions about the stability of steady states in most cases cannot be drawn solely on the basis of whether these states can be calculated using a time-dependent solver or not.

Acknowledgment: The work was supported by FCT—Fundação para a Ciência e a Tecnologia of Portugal through the project Pest-OE/UID/FIS/50010/2013.

Appendix A

Kinetic and Transport Coefficients for Modeling Glow Discharge in Argon

The model used for computing results on discharge in argon shown in Figure 1 accounts for several ionization channels, several ionic species, and non-locality of electron transport and kinetics. The system of reactions, data necessary for calculations, and corresponding references are summarized in Table 1 (here T_e is the electron temperature related to $\bar{\varepsilon}$ the average electron energy by the usual relation $T_e = 2\bar{\varepsilon}/3$). Excited states higher than 4 s were assumed to decay instantly into the representative state Ar^*; in other words, the total rate of excitation into higher excited states, which was computed with BOLSIG+, was included in the source term of conservation equation of species Ar^*.

Mobility and diffusion coefficient of atomic ions Ar^+ were evaluated as functions of the reduced electric field by means of the two-temperature displaced-distribution theory.[35] Mobility of molecular ions Ar_2^+ was evaluated by means of an approximation of the measurements[36]: $\mu_{i2} = 7.1 \times 10^{21} m^{-1} V^{-1} s^{-1} / n_n$, where n_n is the density of neutral gas. Diffusion coefficient of molecular ions Ar_2^+ was evaluated by means of Einstein relation with $T_i = 300$ K. Mobility and diffusion coefficient of electrons were

© 2016 WILEY-VCH Verlag GmbH & Co. KGaA, Weinheim

evaluated as functions of the average electron energy $\bar{\varepsilon}$ using BOLSIG+[30] and cross-sections recommended in ref.[31]

Reaction rates for processes of electron impact ionization and excitation from the ground state were evaluated in terms of the Townsend coefficients, which have been computed in terms of $\bar{\varepsilon}$ by means of BOLSIG+[30] and cross-sections recommended in ref.[31] The effective secondary emission coefficient of both ion species was set equal to 0.03. The transport equations for atoms in excited states and excimers were written in the form of Fick's law. The diffusion coefficients were set equal to $10^{-2}m^2s^{-1}$ following[37] (note that this value has little effect on results, which is in accordance with ref.[37]).

The model comprises also the differential equation of conservation of electron energy in the form suggested in ref.,[30] which governs the distribution of the average electron energy $\bar{\varepsilon}$. The electron energy mobility and electron energy diffusion coefficient were evaluated in terms of $\bar{\varepsilon}$ using BOLSIG+ and cross-sections recommended in ref.,[31] the work function of the cathode material was set equal to 4 eV.

Received: July 1, 2016; Revised: September 16, 2016; Accepted: September 28, 2016; DOI: 10.1002/ppap.201600122

Keywords: DC discharges; electrodes; gas discharge modeling

[1] J. van Dijk, K. Peerenboom, M. Jimenez, D. Mihailova, J. van der Mullen, *J. Phys. D: Appl. Phys.* **2009**, *42*, 194012.
[2] P. G. C. Almeida, M. S. Benilov, *Phys. Plasmas* **2013**, *20*, 101613.
[3] M. S. Benilov, *Plasma Sources Sci. Technol.* **2014**, *23*, 054019.
[4] R. Bötticher, W. Bötticher, *J. Phys. D: Appl. Phys.* **2000**, *33*, 367.
[5] L. Dabringhausen, O. Langenscheidt, S. Lichtenberg, M. Redwitz, J. Mentel, *J. Phys. D: Appl. Phys.* **2005**, *38*, 3128.
[6] M. S. Benilov, M. Carpaij, M. D. Cunha, *J. Phys. D: Appl. Phys.* **2006**, *39*, 2124.
[7] A. Lenef, in Proc. Comsol Users Conference **2006** (Boston, Oct. 22–24, 2006), edited by J. Hiller (COMSOL, ISBN 0-9766792-2-1, Boston, MA, USA, 2006) pp. 125–130.
[8] A. Bergner, M. Westermeier, C. Ruhrmann, P. Awakowicz, J. Mentel, *J. Phys. D: Appl. Phys.* **2011**, *44*, 505203.
[9] M. S. Benilov, M. D. Cunha, "On-line tool for simulation of different modes of axially symmetric current transfer to cathodes of high-pressure arc discharges, version 3," **2009**, http://www.arc_cathode.uma.pt/tool
[10] V. A. Shveigert, *Tech. Phys.* **1993**, *38*, 384.
[11] R. S. Islamov, E. N. Gulamov, *IEEE Trans. Plasma Sci.* **1998**, *26*, 7.
[12] S. T. Surzhikov, *Physical and chemical kinetics in gas dynamics* (electronic journal) **2008**, *7*, in Russian. http://chemphys.edu.ru/issues/2008-7/articles/464/
[13] M. S. Mokrov, Y. P. Raizer, *J. Phys. D: Appl. Phys.* **2011**, *44*, 425202.
[14] J. P. Trelles, *Plasma Sources Sci. Technol.* **2013**, *22*, 025017.
[15] T. Callegari, B. Bernecker, J. P. Boeuf, *Plasma Sources Sci. Technol.* **2014**, *23*, 054003.
[16] Bade, W. L., Yos, J. M., *Theoretical and Experimental Investigation of Arc Plasma-Generation Technology. Part II, Vol. 1: A Theoretical and Experimental Study of Thermionic Arc Cathodes. Technical Report No. ASD-TDR-62-729* (Avco Corpora-tion, Wilmington, Mass., USA, **1963**).
[17] M. S. Benilov, *J. Phys. D: Appl. Phys.* **2008**, *41*, 144001 (30pp).
[18] M. S. Benilov, N. A. Almeida, M. Baeva, M. D. Cunha, L. G. Benilova, D. Uhrlandt, *J. Phys. D: Appl. Phys.* **2016**, *49*, 215201.
[19] M. S. Benilov, M. D. Cunha, G. V. Naidis, *Plasma Sources Sci. Technol.* **2005**, *14*, 517.
[20] Y. S. Touloukian, R. W. Powell, C. Y. Ho, P. G. Clemens, *Thermal Conductivity. Metallic Elements and Alloys*, Thermophysical Properties of Matter, vol. *1*. IFI/Plenum, New York-Washington **1970**.
[21] S. W. H. Yih, C. T. Wang, *Tungsten: Sources, Metallurgy, Properties, and Applications*. Plenum Press, New York **1979**.
[22] Y. P. Raizer, *Gas Discharge Physics*. Springer, Berlin **1991**.
[23] M. S. Benilov, *J. Phys. D: Appl. Phys.* **2007**, *40*, 1376.
[24] M. S. Benilov, M. J. Faria, *J. Phys. D: Appl. Phys.* **2007**, *40*, 5083.
[25] P. G. C. Almeida, M. S. Benilov, M. J. Faria, *J. Phys. D: Appl. Phys.* **2011**, *44*, 415203.
[26] S. Lichtenberg, D. Nandelstädt, L. Dabringhausen, M. Redwitz, J. Luhmann, J. Mentel, *J. Phys. D: Appl. Phys.* **2002**, *35*, 1648.
[27] P. G. C. Almeida, M. S. Benilov, M. J. Faria, *Plasma Sources Sci. Technol.* **2010**, *19*, 025019 (13pp).
[28] A. Fiala, L. C. Pitchford, J. P. Boeuf, *Phys. Rev. E* **1994**, *49*, 5607.
[29] R. R. Arslanbekov, V. I. Kolobov, *J. Phys. D: Appl. Phys.* **2003**, *36*, 2986.
[30] G. J. M. Hagelaar, L. C. Pitchford, *Plasma Sources Sci. Technol.* **2005**, *14*, 722.
[31] M. Hayashi, NIFS—Data 72 **2003**.
[32] L. Vriens, A. H. M. Smeets, *Phys. Rev. A* **1980**, *22*, 940.
[33] A. N. Bhoj, M. J. Kushner, *J. Phys. D: Appl. Phys.* **2004**, *37*, 2510.
[34] G. M. Petrov, C. M. Ferreira, Private communication **2010**.
[35] P. G. C. Almeida, M. S. Benilov, G. V. Naidis, *J. Phys. D: Appl. Phys.* **2002**, *35*, 1577.
[36] M. A. Biondi, L. M. Chanin, *Phys. Rev.* **1954**, *94*, 910.
[37] L. C. Pitchford, J. Kang, C. Punset, J. P. Boeuf, *J. Appl. Phys.* **2002**, *92*, 6990.

© 2016 WILEY-VCH Verlag GmbH & Co. KGaA, Weinheim